nature structural & molecular biology

Crystal structure of the thioesterase domain of human fatty acid synthase inhibited by Orlistat

Charles W Pemble IV[1], Lynnette C Johnson[1], Steven J Kridel[2,3] & W Todd Lowther[1,3]

Human fatty acid synthase (FAS) is uniquely expressed at high levels in many tumor types. Pharmacological inhibition of FAS therefore represents an important therapeutic opportunity. The drug Orlistat, which has been approved by the US Food and Drug Administration, inhibits FAS, induces tumor cell–specific apoptosis and inhibits the growth of prostate tumor xenografts. We determined the 2.3-Å-resolution crystal structure of the thioesterase domain of FAS inhibited by Orlistat. Orlistat was captured in the active sites of two thioesterase molecules as a stable acyl-enzyme intermediate and as the hydrolyzed product. The details of these interactions reveal the molecular basis for inhibition and suggest a mechanism for acyl-chain length discrimination during the FAS catalytic cycle. Our findings provide a foundation for the development of new cancer drugs that target FAS.

The human FAS protein is specifically upregulated in many tumors, including, but not limited to, those from prostate and breast tissue[1]. FAS expression also correlates with poor prognosis, suggesting that FAS activity is advantageous to cancer cells. The natural product cerulenin and its synthetic analog C75 have been shown to inhibit FAS activity, induce apoptosis and inhibit tumor growth in xenograft and transgenic models of cancer[2–5]. These studies and RNA interference experiments have verified FAS as a key anticancer target[6]. Orlistat, a US Food and Drug Administration (FDA)-approved β-lactone–containing drug, inhibits the thioesterase domain of FAS, induces endoplasmic reticulum stress and tumor cell death, inhibits tumor growth and prevents angiogenesis[7–9]. Therefore, we set out to determine how Orlistat inhibits the FAS thioesterase, in an effort to provide a basis for the development of new therapeutic agents.

The thioesterase is the seventh functional domain of the 270-kDa FAS polypeptide (**Fig. 1a**)[10,11]. The remaining domains of the FAS homodimer coordinate to primarily synthesize *de novo* the 16-carbon (C_{16}) fatty acid palmitate (**Supplementary Fig. 1** online). The thioesterase domain catalyzes the termination step by hydrolyzing the thioester bond between palmitate and the 4′-phosphopantetheine moiety of the acyl-carrier protein (ACP) domain[12–14]. The release of the thioesterase from FAS by limited proteolysis, however, results in the production of fatty acids containing 20 to 22 carbons[15]. Thus, the thioesterase domain is essential in regulating the length of the fatty acid chain.

The structural origins behind the FAS reaction and substrate specificity have been investigated by several groups. Chemical cross-linking, complementation and cryo-EM studies have led to proposals of the domain interactions within FAS[10,11,16,17]. The recent crystal structure of porcine FAS has resolved many of the discrepancies between these proposals and provided remarkable insight into the shuttling of the growing fatty acid chain between the domains[18]. Notably, the ACP and thioesterase domains are not visible in the porcine FAS structure, suggesting that they are inherently flexible relative to the core of FAS.

The crystal structure of the recombinant thioesterase domain has previously been solved in the absence of ligands[19]. We herein describe the 2.3-Å-resolution crystal structure of the thioesterase in complex with Orlistat (**Fig. 1b**) in two forms: an unusually stable acyl-enzyme intermediate and the hydrolyzed product. These structures show that Orlistat is a substrate of the thioesterase domain, which is comprised of two subdomains (**Fig. 1c**), with the Ser2308-His2481-Asp2338 catalytic triad located in subdomain A. A surface loop within this canonical α/β-hydrolase fold is extended to form the unique, α-helical subdomain B. An analysis of site-directed mutants and molecular modeling using a substrate-analog inhibitor have also suggested that only about four to six carbon atoms at the terminus of palmitate fit into a cavity at the interface of the two subdomains[19]. In the present study, the C_{16} core of Orlistat is reminiscent of palmitate and binds almost exclusively to a hydrophobic surface channel generated by subdomain B and not the interface cavity. These observations provide a clear mechanism for Orlistat inhibition, a rationale for substrate specificity and a description of possible ACP domain interactions. The resulting molecular blueprint will enable future biochemical studies and the design of anticancer compounds with improved potency, selectivity and bioavailability.

[1]Center for Structural Biology and Department of Biochemistry, [2]Department of Cancer Biology and [3]Comprehensive Cancer Center of Wake Forest University, Wake Forest University School of Medicine, Medical Center Boulevard, Winston-Salem, North Carolina 27157, USA. Correspondence should be addressed to W.T.L. (tlowther@wfubmc.edu).

Received 30 March; accepted 30 May; published online 8 July 2007; doi:10.1038/nsmb1265

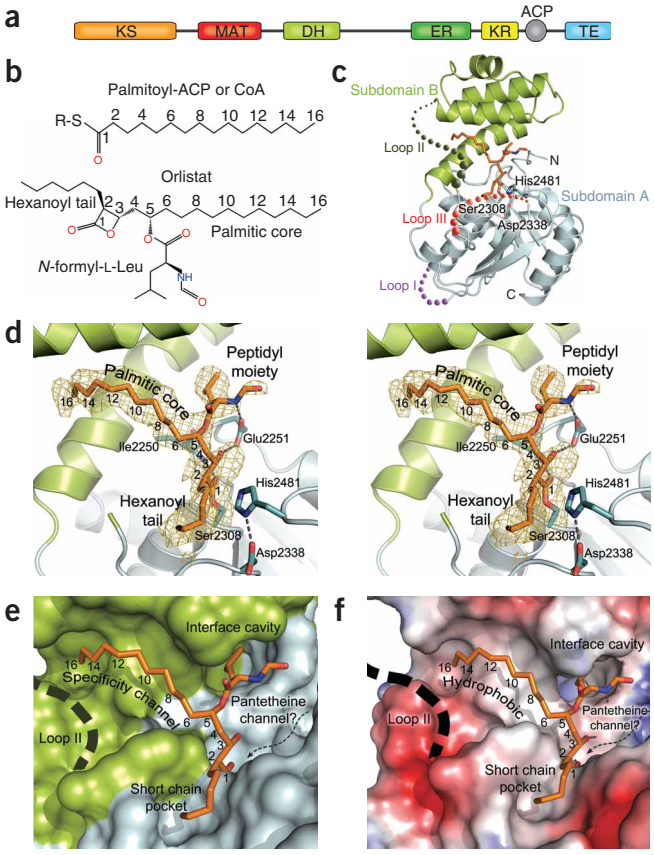

Figure 1 FAS and the covalent thioesterase–Orlistat complex. (**a**) Domain organization of FAS and its seven catalytic activities: β-ketoacyl synthase (KS), acetyl/malonyl-CoA transferase (MAT), β-hydroxyacyl dehydratase (DH), enoyl reductase (ER), β-ketoacyl reductase (KR), acyl-carrier protein (ACP) and thioesterase (TE). (**b**) Structural comparison between FAS substrates and Orlistat. R-S represents the thioester-linked 4′-phosphopantetheine moiety attached to either the ACP domain or CoA. (**c**) Overall fold of the thioesterase domain with Orlistat bound. The topology of the thioesterase within the Orlistat complex shares similarities with the apoenzyme structure[19]; superposition of the Cα carbon atoms results in an r.m.s. deviation of 3.5 Å. (**d**) Orlistat bound in the active site of chain A. The Orlistat scaffold is divided into three fragments: peptidyl moiety (*N*-formyl-L-leucine substituent extending off the C5 carbon atom), palmitic core and hexanoyl tail (C2 substituent). Shown covering Orlistat and Ser2308 is the $F_o - F_c$ simulated-annealing omit electron density contoured at 3 σ. (**e**,**f**) Molecular (**e**) and electrostatic (**f**) surface representations colored to reflect the subdomain division (as in **c**) and electrostatic potential, respectively. The potential contours in **f** are shown on a scale from +130 (blue) to –40 k_bTe^{-1} (red); white indicates no charge.

RESULTS

Thioesterase domain–Orlistat structure overview

The human thioesterase domain–Orlistat complex crystallized with two molecules (chains A and B) present in the asymmetric unit (**Table 1**), stabilized by a DTT molecule and several water molecules bound at the interface (**Supplementary Fig. 2** online). Each thioesterase molecule contained a different form of Orlistat: a covalent acyl-enzyme intermediate or the hydrolyzed product. The monomeric thioesterase domain is divided into subdomains A and B (**Fig. 1c**). Subdomain A contains a central, mostly parallel β-sheet made up of seven strands. Flanking the half barrel sheet are four α-helices, which complete the canonical α/β-hydrolase fold. Like other α/β-hydrolases, the thioesterase domain contains a loop insertion near the catalytic Ser2308-His2481-Asp2338 triad. In this case, however, the loop insertion is an entire domain (subdomain B) that adopts a unique, helical tertiary structure. Three additional loop regions had poor electron density and were not included in the model: loop I (residues 2326–2328, missing in chain A only) connects α-helix 4 (α4) to β-strand 5 (β5), forming a surface loop on the underside of the α/β domain, away from the active site; loop II (residues 2344–2360) bridges subdomain A and subdomain B; and loop III (residues 2450–2460) is near the catalytic triad linking β6 to β7.

Orlistat acyl-enzyme intermediate

The electron density for chain A (**Fig. 1d**) shows that Orlistat binds in an extended conformation with covalent attachment to Ser2308 of the catalytic triad within subdomain A. A closer inspection of the Orlistat adduct indicates that it is a stabilized acyl-enzyme intermediate (that is, a stable ester linkage). Moreover, the retention of the *S* configuration at all four chiral centers is consistent with a nucleophilic attack at the carbonyl C1 position and not the C3 position of the β-lactone ring. These observations are in agreement with previously reported mass spectrometry data for Orlistat hydrolyzed by porcine pancreatic lipase[20,21].

In addition to the Ser2308 adduct, the various chemical moieties of Orlistat (**Fig. 1b**) extensively interact with the surface of the thioesterase (**Fig. 1e**,**f**). The *N*-formyl-L-leucine moiety (or peptidyl moiety) interacts with a cavity at the interface that is also evident in the apoenzyme structure[19]. The 16-carbon palmitic core binds in a hydrophobic channel that we term the specificity channel, and the hexanoyl tail binds in a pocket that we term the short-chain pocket. These extensive interactions correlate well with the observed potency of Orlistat against the recombinant thioesterase domain and FAS in tumor cells[7,22].

The peptidyl moiety of Orlistat binds in the interface cavity, which is generated by residues from both subdomains (**Fig. 2a**). The L-leucine component interacts primarily with residues on the rim of the cavity, including Leu2222, Ile2250, Gln2374, Phe2370, Phe2371, Phe2375 and Phe2423. Glu2251 forms a hydrogen bond to the nitrogen atom of the *N*-formylamide group. The distal chamber of the cavity is filled with several water molecules held in place by a hydrogen-bonding network that includes Lys2426. The palmitic core of Orlistat binds a predominantly hydrophobic specificity channel (**Fig. 1f** and **Fig. 2b**) comprised of residues almost exclusively from subdomain B: Ala2363, Glu2366, Ala2367, Phe2370, Phe2423, Tyr2424, Leu2427, Arg2428 and Glu2431. Residues Ile2250 and Tyr2309 from subdomain A are the exceptions. The majority of the former residues are conserved among FAS homologs (**Supplementary Fig. 3** online). The main chain nitrogen atoms of the latter two residues form the oxyanion hole and weakly hydrogen-bond with the C1 carbonyl oxygen atom of Orlistat. Ala2363 and Tyr2424 provide a constriction at the end of the channel. Glu2431 and Arg2428 are located at the far end of the channel and provide an electrostatic barrier near the terminal carbon atom of the C_{16} acyl chain of Orlistat. The hexanoyl tail, which extends off the C2 carbon atom of Orlistat, interacts with Gly2339, Thr2342, Tyr2343 and Tyr2462 (**Fig. 2c**). Moreover, this functional group packs against His2481 of the catalytic triad.

Hydrolyzed Orlistat

The electron density for hydrolyzed Orlistat in chain B of the complex (**Fig. 3a**) indicates that the acyl-enzyme intermediate has collapsed to

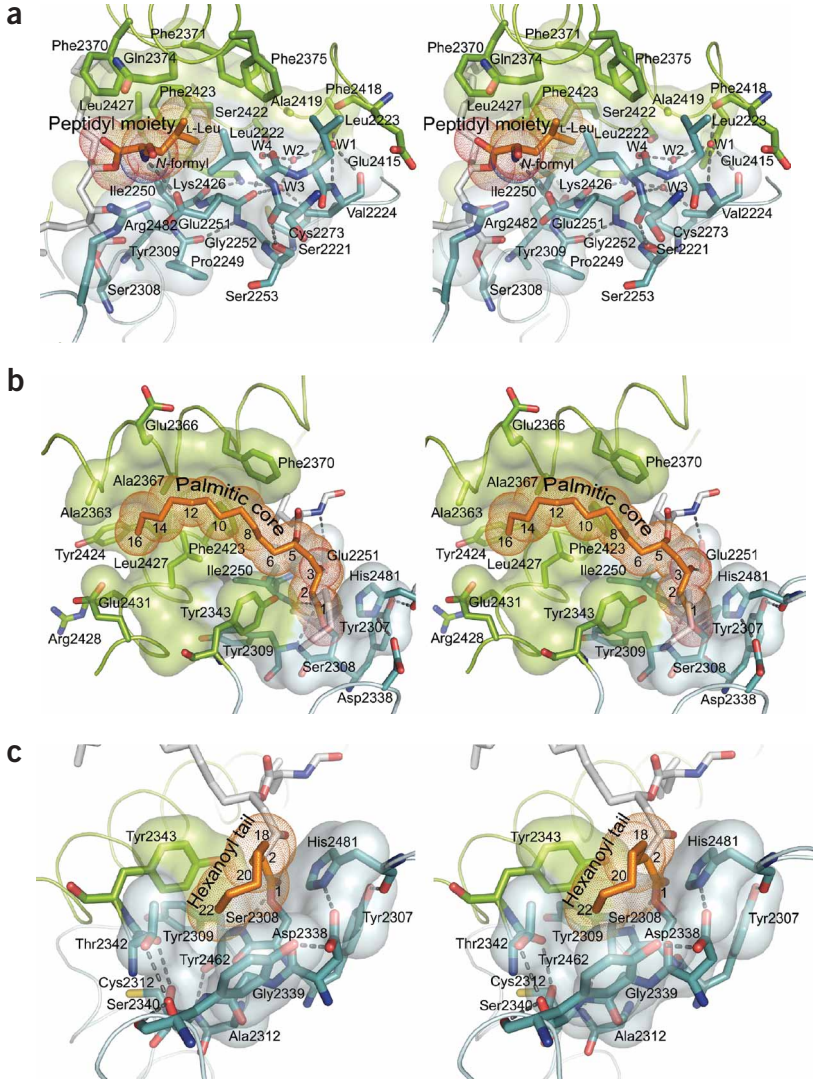

Figure 2 Detailed interactions between the thioesterase domain and Orlistat chemical moieties. Shown are atomic surfaces of only those residues that contribute to Orlistat binding in AREAIMOL calculations. (**a**) Stereo view (oriented 90° from **Fig. 1d–f**) of the bound peptidyl moiety within the interface cavity. Gray dashed lines denote putative hydrogen bonds. Water molecules are labeled W1–W4. The nitrogen atom of the *N*-formyl group is 3.2 Å from the Oε1 atom of Glu2251. (**b**) Stereo view of the palmitic core packing onto the hydrophobic specificity channel. (**c**) Stereo view of the hexanoyl tail binding into the hydrophobic short-chain pocket.

form a product containing a carboxylic acid at the C1 position. This finding is most probably a consequence of the 3-week crystallization period, as there are minor structural differences between the thioesterase molecules and no apparent crystal-lattice effects. The C1 position of the product is also shifted ~4 Å (**Fig. 3b**) relative to the covalent adduct, and two intervening water molecules now occupy the oxyanion hole. The position of the peptidyl moiety is altered slightly, and the palmitic core has shifted in register by approximately two carbon units (**Fig. 3c**). This shift places the terminal carbon atom closer to the hydrophobic constriction and charge barrier created by Ala2363, Tyr2424, Glu2431 and potentially Arg2428. The hexanoyl C2 substituent has also moved considerably (~9 Å), and Tyr2343 of loop II has repositioned to form a hydrogen bond with the new C1 carboxylate group of Orlistat. The interactions of the covalent adduct and hydrolyzed Orlistat also suggest that the 4′-phosphopantetheine arm of the ACP domain docks into another channel adjacent to Ser2308 (**Fig. 1e,f**) lined with the conserved residues Val2256, Tyr2307, Arg2482 and Leu2485 (**Supplementary Fig. 3**).

DISCUSSION

Although Orlistat is currently approved by the FDA for obesity management, the antitumor effects of Orlistat are clearly associated with FAS inhibition[7–9]. The possibility of targeting the thioesterase domain of FAS with Orlistat or other compounds prompted us to characterize the molecular basis for this important interaction. Our observations provide structural confirmation that nucleophilic attack occurs at the C1 carbonyl atom of Orlistat (**Fig. 1b**), leading to the formation of an unusually stable acyl-enzyme intermediate (**Fig. 1d**). Therefore, the Orlistat covalent complex will serve as a model for the interactions and reactivity of presumably all β-lactone–containing compounds designed for the thioesterase domain[22,23]. Moreover, the C_{16} hydrocarbon backbone of Orlistat mimics palmitate, enabling a rationalization of substrate specificity.

A previous study has docked a molecular model of the C_{16}-containing inhibitor hexadecyl sulfonyl fluoride onto the apoenzyme form of the thioesterase domain[19]. The authors proposed that only about four to six carbon atoms at the terminus of a C_{16} or C_{18} substrate fit into the interface cavity. In contrast, we found that the C_{16} palmitate-like moiety of Orlistat is bound in an extended conformation to a hydrophobic specificity channel ~23 Å in length (**Fig. 1c–e**), and the *N*-formyl-L-leucine moiety packs into the interface cavity. We also identified a new short chain–binding pocket, which surrounds the hexanoyl tail that extends off the C2 position of Orlistat. Notably, if one counts the number of carbons from the C1 atom of Orlistat to the end of the L-leucine side chain (**Fig. 2a**), the aliphatic chain is 11 carbons in length, and the limited volume and depth of the interface cavity (219 $Å^3$ and ~10–14 Å, respectively) suggest that C_{16} substrates cannot be accommodated. The reduced activity of some mutants in this region is most probably a consequence of prying the subdomains apart. For example, the mutation of Ile2250, Ala2419 and Phe2423 to larger amino acid residues, as described[19], would be especially detrimental, as the spatial relationships between the catalytic triad, oxyanion hole and specificity channel would be changed. Furthermore, mutation of Ile2250 to a bulky residue probably occludes the oxyanion hole[19]. Electrostatic calculations (**Fig. 1f**) suggest that the presence of Lys2426 and a series of water molecules in the interface pocket (**Fig. 2a**) would also deter the binding of aliphatic substrates.

The binding of palmitoyl substrates to the hydrophobic specificity channel of the thioesterase domain is supported by two additional

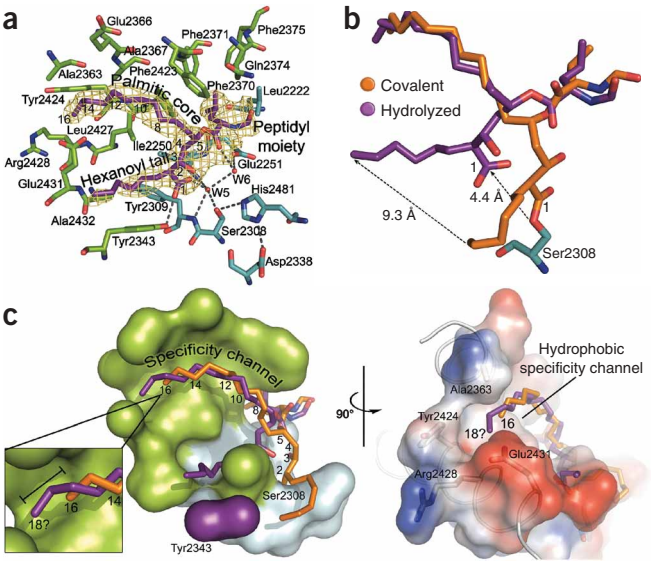

Figure 3 Metabolized Orlistat interactions and chain-length selectivity. (**a**) Hydrolyzed Orlistat within the active site of chain B, depicted as in **Figure 2**. Shown covering the Orlistat product is the $F_o - F_c$ simulated-annealing omit electron density contoured at 3 σ. (**b**) Superposition of the two metabolized forms of Orlistat. (**c**) Molecular (left) and electrostatic surface (right, as in **Fig. 1f**) representations of the covalent and hydrolyzed Orlistat complexes. Upon hydrolysis of the acyl-enzyme intermediate, Tyr2343 of loop II moves down to hydrogen-bond with the C1 carboxyl group of Orlistat. The resulting change in the surface is indicated in purple. A shift in register relative to the covalent intermediate extends the hydrolyzed product two carbon units (indicated by bar in inset) beyond C_{16}, mimicking the chain length of C_{18}.

observations. First, Orlistat is a substrate that forms an acyl-enzyme intermediate (**Fig. 1d**), which ultimately collapses to form the product (**Fig. 3a**). Second, the almost exclusive binding of the palmitic core to subdomain B is consistent with the observed structural plasticity of α/β-hydrolases in this region. Surface loop insertions into the common α/β core (**Fig. 1c**) have made the α/β-hydrolase superfamily among the most functionally diverse of protein families[24]. Although catalysis occurs via the same chemistry in all α/β-hydrolases, a variety of substrates of different sizes are cleaved. Therefore, the thioesterase–Orlistat complexes provide evidence that the role of the inserted α-helical subdomain is to provide a hydrophobic surface channel for substrate selection. The presence of Glu2431 and Arg2428 and the constriction caused by Ala2363 and Tyr2424 (**Fig. 2b** and **Fig. 3c**) most probably generate the preference for C_{16}-containing substrates such as Orlistat. The translation of the Orlistat product complex that we observed is consistent with the ability of the thioesterase domain to catalyze the release of C_{18} substrates[12–14].

Figure 4 presents a model for the molecular basis of inhibition by β-lactone–containing compounds and of the hydrolysis of substrates. Although the binding mode of the β-lactone form of Orlistat is not known, we postulate that the oxygen atom of the C1 carbonyl group is bound in the oxyanion hole (**Fig. 4a**). The interactions with the specificity channel provide the correct register, leading to the attack of Ser2308 to form the acyl-enzyme intermediate and subsequent opening of the β-lactone ring (**Fig. 4b**). This intermediate is stabilized by the oxyanion hole and a hydrogen bond to Glu2251. Most importantly, the hexanoyl tail that extends off the C2 position of Orlistat packs against His2481 (**Fig. 2c**). This interaction may prevent the activation of a water molecule that, for naturally occurring substrates, would result in the immediate hydrolysis of the intermediate.

Given time, however, the hexanoyl tail of Orlistat moves enough to allow water activation by His2481, and the Orlistat adduct undergoes deacylation (**Fig. 4c**). The peptidyl moiety seems to serve as a key determinant in anchoring the Orlistat product to the interface cavity, as only minor changes in this moiety were observed relative to the acyl-enzyme intermediate. In contrast, the hexanoyl-tail and palmitic-core fragments shift considerably to the left, which allows two intervening water molecules to bind, one of which is in the oxyanion hole. With these movements, the hexanoyl tail vacates the short-chain pocket and establishes new interactions with Tyr2309, Tyr2343 and Ala2432. Notably, the portion of loop II that is visible by crystallography undergoes a structural rearrangement (**Fig. 3c**) to form hydrophobic contacts and a hydrogen bond between the hydroxyl group of Tyr2343 and the new C1 carboxylate group of Orlistat.

Our thioesterase–Orlistat complexes also provide a rationale for chain-length selectivity during the fatty acid synthesis cycle

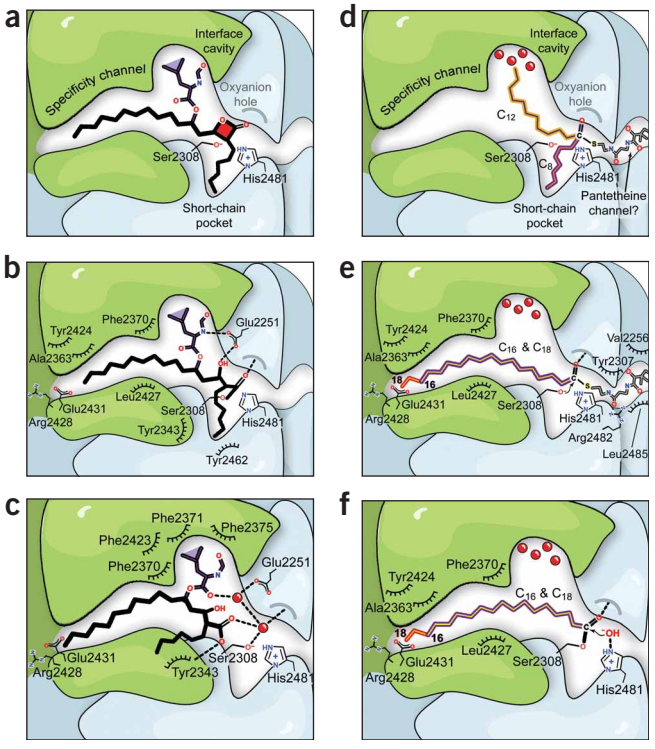

Figure 4 Molecular basis for Orlistat-mediated inhibition and substrate selectivity. (**a**) Proposed interactions with the intact β-lactone form of Orlistat. (**b**) The Orlistat acyl-enzyme intermediate. Semicircles with tick marks indicate van der Waals interactions. (**c**) Hydrolyzed Orlistat and its movements. (**d**) Hypothetical mechanism for chain-length sampling. Red spheres represent four water molecules involved in an intricate hydrogen-bonding network within the interface cavity (**Fig. 2a**); for simplicity, waters are omitted in **a**–**c**. The 4′-phosphopantetheine arm (gray stick model) of ACP is shown bound to the putative pantetheine channel. Representative growing acyl chains measuring 8 and 12 carbons in length (extrapolated from the Orlistat covalent complex) are shown binding transiently to the short-chain pocket and interface cavity, respectively. (**e**) Selection of C_{16} and C_{18} substrates and formation of the Michaelis complex. (**f**) Hydrolysis of the acyl-enzyme intermediate.

(**Supplementary Fig. 1**). During the FAS reaction, the acyl chain grows by two carbon units. One potential scenario for the selection of substrates is that the interactions of the thioesterase and ACP domains with the other domains of FAS influence the loading of substrate into the thioesterase domain. This domain can release palmitate and stearate (C_{18}) when attached to ACP or CoA[10–14]. The proteolytic release of the thioesterase from FAS, however, results in the synthesis of C_{20} and C_{22} fatty acids[15]. Therefore, the thioesterase seems to be a crucial determinant of substrate selection. These observations suggest a second scenario, where FAS reaction intermediates sample the short-chain pocket and interface cavity (**Fig. 4d**). It appears that these regions are able to accommodate only short- to medium-length fatty acids (of 4 to 12 carbons). The thioester moiety of such potential thioesterase substrates is probably not positioned correctly for catalysis to occur[25]. C_{16} and C_{18} substrates, however, would extend to the end of the specificity channel (**Fig. 4e**) like the palmitic core of Orlistat, thus positioning the scissile bond appropriately for catalysis. Ala2363, Tyr2424, Arg2428 and Glu2431 at the far end of this channel appear to be responsible for generating the barrier to longer substrates. In contrast to the slow hydrolysis of the Orlistat acyl-enzyme intermediate, His2481 facilitates the rapid hydrolysis of palmitoyl or stearoyl acyl-enzyme intermediates (**Fig. 4f**).

In this model, substrates that bind the specificity channel should be no shorter than 16 carbons, to correctly orient the thioester bond relative to Ser2308 for nucleophilic attack (**Fig. 4e**). In this context, the 4′-phosphopantetheine arm of the ACP domain or CoA may also help to position the substrate correctly for catalysis. We identified a putative binding channel adjacent to Orlistat and the catalytic triad. The proximity of the flexible loop II to the catalytic triad, short-chain pocket and specificity channel also suggests that loop II may participate in substrate loading within the macromolecular FAS dimer. These insights combined may be useful for orienting the ACP and thioesterase domains within the available EM structures and future crystal structures of intact FAS[16,17]. We envision that the FAS thioesterase–Orlistat complexes will stimulate the design, synthesis, optimization and testing of new compounds for cancer therapy and additional functional studies concerning FAS biochemistry and substrate specificity.

METHODS

Protein expression and purification. The thioesterase domain of human FAS (residues 2200–2510) was cloned as previously described[7]. The domain was subcloned into the pET15b (Novagen) vector containing an N-terminal His_6 tag with an intervening thrombin cleavage site. The thioesterase was overexpressed in C41(DE3) *Escherichia coli* grown in a 10-l fermentor at 37 °C and induced by 0.5 mM IPTG at 25 °C when the cells reached an A_{600} of 1. The cells were harvested after 4 h and lysed, and the supernatant was passed over a nickel–nitrilotriacetic acid affinity column (Qiagen). The desired fractions were immediately treated with 2 mM EDTA and 15 mM DTT and dialyzed overnight at 4 °C against 20 mM HEPES (pH 8.5), 1 mM EDTA and 1 mM DTT. The protein was further purified using a DEAE Macro-Prep column (Bio-Rad) with a linear gradient from 0 to 1 M NaCl in 20 mM HEPES (pH 8.5), 1 mM EDTA and 1 mM DTT. The thioesterase was concentrated to 2 mg ml^{-1} and treated with 0.1 U mg^{-1} biotinylated thrombin (Novagen) at 16 °C overnight to remove the His tag. His-tag cleavage was confirmed by MALDI-TOF mass spectrometry, and the biotinylated thrombin was removed by the addition of streptavidin agarose (Novagen). To obtain the preformed covalent thioesterase–Orlistat complex, a reaction mixture containing the thioesterase domain and a 60-fold molar excess of Orlistat (β-lactone form) was incubated at 20 °C for 1 h. The completion of adduct formation was confirmed by electrospray mass spectrometry. The resulting complex was purified away from excess Orlistat and buffer exchanged using a Superdex 200 gel-filtration column (GE Healthcare) equilibrated with 20 mM HEPES (pH 7.5), 100 mM NaCl and 1 mM DTT. The complex was concentrated to 17 mg ml^{-1}, flash-frozen in liquid nitrogen and stored at –80 °C.

Table 1 Data collection and refinement statistics

	Orlistat complexes
Data collection	
Space group	$P2_1$
Cell dimensions	
a, *b*, *c* (Å)	41.9, 94.3, 69.7
α, β, γ (°)	90.0, 95.8, 90.0
Resolution (Å)	39.0–2.3 (2.38–2.30)
R_{merge}	0.06 (0.23)
$I / \sigma I$	17.0 (6.2)
Completeness (%)	96.0 (76.2)
Redundancy	7.1 (6.2)
Refinement	
Resolution (Å)	39.0–2.3
No. reflections	21,850
R_{work} / R_{free}	22.5 / 27.3
No. atoms	
Protein	4,016
Orlistat covalent	35
Orlistat hydrolyzed	36
DTT	8
Water	53
B-factors	
Protein	36.6
Orlistat covalent	60.2
Orlistat hydrolyzed	67.1
Water	30.6
R.m.s. deviations	
Bond lengths (Å)	0.01
Bond angles (°)	1.27

Data were collected from a single crystal. Values in parentheses are for the highest-resolution shell.

Crystallization and structure determination. Crystals of the thioesterase–Orlistat complex were grown using hanging drop vapor diffusion. Equal volumes of protein (6 mg ml^{-1} in 20 mM HEPES (pH 7.5), 100 mM NaCl and 30 mM DTT) and precipitant solution were mixed and equilibrated at 15 °C against well solutions containing 100 mM sodium dihydrogen phosphate (pH 4.25), 20%–26% (w/v) PEG 3,350 and 30 mM DTT. Crystals were transferred to a synthetic mother-liquor solution containing 50 mM sodium dihydrogen phosphate (pH 4.25), 32% (w/v) PEG 3,350, 30 mM DTT and 25% (v/v) of the cryoprotectant ethylene glycol before cryocooling to –170 °C. X-ray diffraction data ($\lambda = 1.0$ Å) were collected at the National Synchrotron Light Source, Brookhaven National Laboratory, on beamline X12C. Data were indexed and scaled to 2.3-Å resolution using the d*TREK suite[26] (**Table 1**). The structure was solved by molecular replacement using PHASER[27] with the native, uncomplexed structure of the thioesterase domain (PDB 1XKT)[19] as a search model. The initial model was manually rebuilt using COOT[28]. Iterative structure refinement was carried out using a combination of CNS[29] and REFMAC5 (ref. 30). DTT molecular topologies were obtained using the HIC-Up server[31]. The molecular coordinates and topologies of both the covalent and hydrolyzed forms of Orlistat were generated using the PRODRG2 server[32]. The final refined model of the thioesterase–Orlistat complex had R_{work} and R_{free} values of 22.5% and 27.3%, respectively. The structure was validated using the MOLPROBITY server[33], which reported 96.8% of the residues in the Ramachandran favored regions, 2.6% in the allowed regions and 0.6% as outliers. The thioesterase domain contains several loop regions that have intrinsic mobility. As a result, a protein model could not be built for the following disordered regions: residues 2326–2328 (loop I,

chain B only), 2344–2360 (loop II, both chains), 2450–2460 (loop III, both chains) and residues 2200–2220 and 2502–2510 on the N and C termini, respectively. AREAIMOL[34] was used to identify surface residues that interact with Orlistat through either hydrophobic or polar contacts. Other surface calculations were performed using CASTP[35].

Illustrations. All structural illustrations were generated using PyMOL[36].

Accession codes. Protein Data Bank: Coordinates and structure factors have been deposited with accession code 2PX6.

Note: Supplementary information is available on the Nature Structural & Molecular Biology website.

ACKNOWLEDGMENTS

This work was supported by developmental funds from Wake Forest University School of Medicine, the Kulynych Interdisciplinary Cancer Research Fund, the US Department of Defense Prostrate Cancer Research Program (W81XWH-05-1-0065) and the US National Institutes of Health, National Cancer Institute (R01 CA114104) to S.J.K and W.T.L. The authors' views and opinions do not reflect those of the US Army or the Department of Defense. The authors thank T. Hollis and D.A. Lehtinen for assistance in collecting diffraction data on beamline x12c at the National Synchrotron Light Source, Brookhaven National Laboratory. The National Synchrotron Light Source is supported by funds from the US Department of Energy, Office of Science, Office of Basic Energy Sciences under contract no. DE-AC02-98CH10886. We also thank J.D. Schmitt for insightful discussions and comments on the manuscript.

AUTHOR CONTRIBUTIONS

C.W.P., S.J.K. and W.T.L. designed the experiments and interpreted the structure; S.J.K. generated the expression clone; C.W.P. and L.C.J. performed all protein expression, purification and crystallization; C.W.P. and W.T.L. contributed to structure solution and refinement; all authors contributed to manuscript preparation.

COMPETING INTERESTS STATEMENT

The authors declare no competing financial interests.

Published online at http://www.nature.com/nsmb/
Reprints and permissions information is available online at http://npg.nature.com/reprintsandpermissions

1. Kuhajda, F.P. Fatty acid synthase and cancer: new application of an old pathway. *Cancer Res.* **66**, 5977–5980 (2006).
2. Kuhajda, F.P. *et al.* Synthesis and antitumor activity of an inhibitor of fatty acid synthase. *Proc. Natl. Acad. Sci. USA* **97**, 3450–3454 (2000).
3. Pizer, E.S. *et al.* Inhibition of fatty acid synthesis delays disease progression in a xenograft model of ovarian cancer. *Cancer Res.* **56**, 1189–1193 (1996).
4. Pizer, E.S. *et al.* Increased fatty acid synthase as a therapeutic target in androgen-independent prostate cancer progression. *Prostate* **47**, 102–110 (2001).
5. Alli, P.M., Pinn, M.L., Jaffee, E.M., McFadden, J.M. & Kuhajda, F.P. Fatty acid synthase inhibitors are chemopreventive for mammary cancer in neu-N transgenic mice. *Oncogene* **24**, 39–46 (2005).
6. De Schrijver, E., Brusselmans, K., Heyns, W., Verhoeven, G. & Swinnen, J.V. RNA interference-mediated silencing of the fatty acid synthase gene attenuates growth and induces morphological changes and apoptosis of LNCaP prostate cancer cells. *Cancer Res.* **63**, 3799–3804 (2003).
7. Kridel, S.J., Axelrod, F., Rozenkrantz, N. & Smith, J.W. Orlistat is a novel inhibitor of fatty acid synthase with antitumor activity. *Cancer Res.* **64**, 2070–2075 (2004).
8. Browne, C.D., Hindmarsh, E.J. & Smith, J.W. Inhibition of endothelial cell proliferation and angiogenesis by orlistat, a fatty acid synthase inhibitor. *FASEB J.* **20**, 2027–2035 (2006).
9. Little, J.L., Wheeler, F.B., Fels, D., Koumenis, C. & Kridel, S.J. Fatty acid synthase inhibitors induce endoplasmic reticulum stress in tumor cells. *Cancer Res.* **67**, 1262–1269 (2007).
10. Chirala, S.S. & Wakil, S.J. Structure and function of animal fatty acid synthase. *Lipids* **39**, 1045–1053 (2004).
11. Smith, S., Witkowski, A. & Joshi, A.K. Structural and functional organization of the animal fatty acid synthase. *Prog. Lipid Res.* **42**, 289–317 (2003).
12. Pazirandeh, M., Chirala, S.S., Huang, W.Y. & Wakil, S.J. Characterization of recombinant thioesterase and acyl carrier protein domains of chicken fatty acid synthase expressed in *Escherichia coli*. *J. Biol. Chem.* **264**, 18195–18201 (1989).
13. Lin, C.Y. & Smith, S. Properties of the thioesterase component obtained by limited trypsinization of the fatty acid synthetase multienzyme complex. *J. Biol. Chem.* **253**, 1954–1962 (1978).
14. Joshi, A.K., Witkowski, A., Berman, H.A., Zhang, L. & Smith, S. Effect of modification of the length and flexibility of the acyl carrier protein-thioesterase interdomain linker on functionality of the animal fatty acid synthase. *Biochemistry* **44**, 4100–4107 (2005).
15. Singh, N., Wakil, S.J. & Stoops, J.K. On the question of half- or full-site reactivity of animal fatty acid synthetase. *J. Biol. Chem.* **259**, 3605–3611 (1984).
16. Asturias, F.J. *et al.* Structure and molecular organization of mammalian fatty acid synthase. *Nat. Struct. Mol. Biol.* **12**, 225–232 (2005).
17. Brink, J. *et al.* Experimental verification of conformational variation of human fatty acid synthase as predicted by normal mode analysis. *Structure* **12**, 185–191 (2004).
18. Maier, T., Jenni, S. & Ban, N. Architecture of mammalian fatty acid synthase at 4.5 Å resolution. *Science* **311**, 1258–1262 (2006).
19. Chakravarty, B., Gu, Z., Chirala, S.S., Wakil, S.J. & Quiocho, F.A. Human fatty acid synthase: structure and substrate selectivity of the thioesterase domain. *Proc. Natl. Acad. Sci. USA* **101**, 15567–15572 (2004).
20. Hadvary, P., Sidler, W., Meister, W., Vetter, W. & Wolfer, H. The lipase inhibitor tetrahydrolipstatin binds covalently to the putative active site serine of pancreatic lipase. *J. Biol. Chem.* **266**, 2021–2027 (1991).
21. Luthi-Peng, Q., Marki, H.P. & Hadvary, P. Identification of the active-site serine in human pancreatic lipase by chemical modification with tetrahydrolipstatin. *FEBS Lett.* **299**, 111–115 (1992).
22. Ma, G. *et al.* Total synthesis and comparative analysis of orlistat, valilactone, and a transposed orlistat derivative: inhibitors of fatty acid synthase. *Org. Lett.* **8**, 4497–4500 (2006).
23. Purohit, V.C., Richardson, R.D., Smith, J.W. & Romo, D. Practical, catalytic, asymmetric synthesis of beta-lactones via a sequential ketene dimerization/hydrogenation process: inhibitors of the thioesterase domain of fatty acid synthase. *J. Org. Chem.* **71**, 4549–4558 (2006).
24. Nardini, M. & Dijkstra, B.W. Alpha/beta hydrolase fold enzymes: the family keeps growing. *Curr. Opin. Struct. Biol.* **9**, 732–737 (1999).
25. Kraut, J. Serine proteases: structure and mechanism of catalysis. *Annu. Rev. Biochem.* **46**, 331–358 (1977).
26. Pflugrath, J.W. The finer things in X-ray diffraction data collection. *Acta Crystallogr. D Biol. Crystallogr.* **55**, 1718–1725 (1999).
27. McCoy, A.J., Grosse-Kunstleve, R.W., Storoni, L.C. & Read, R.J. Likelihood-enhanced fast translation functions. *Acta Crystallogr. D Biol. Crystallogr.* **61**, 458–464 (2005).
28. Emsley, P. & Cowtan, K. Coot: model-building tools for molecular graphics. *Acta Crystallogr. D Biol. Crystallogr.* **60**, 2126–2132 (2004).
29. Brunger, A.T. *et al.* Crystallography & NMR system: a new software suite for macromolecular structure determination. *Acta Crystallogr. D Biol. Crystallogr.* **54**, 905–921 (1998).
30. Murshudov, G.N., Vagin, A.A. & Dodson, E.J. Refinement of macromolecular structures by the maximum-likelihood method. *Acta Crystallogr. D Biol. Crystallogr.* **53**, 240–255 (1997).
31. Kleywegt, G.J. Crystallographic refinement of ligand complexes. *Acta Crystallogr. D Biol. Crystallogr.* **63**, 94–100 (2007).
32. Schuttelkopf, A.W. & van Aalten, D.M. PRODRG: a tool for high-throughput crystallography of protein-ligand complexes. *Acta Crystallogr. D Biol. Crystallogr.* **60**, 1355–1363 (2004).
33. Davis, I.W., Murray, L.W., Richardson, J.S. & Richardson, D.C. MOLPROBITY: structure validation and all-atom contact analysis for nucleic acids and their complexes. *Nucleic Acids Res.* **32**, 615–619 (2004).
34. Collaborative Computational Project, Number 4. The CCP4 suite: programs for protein crystallography. *Acta Crystallogr. D Biol. Crystallogr.* **50**, 760–763 (1994).
35. Binkowski, T.A., Naghibzadeh, S. & Liang, J. CASTp: computed atlas of surface topography of proteins. *Nucleic Acids Res.* **31**, 3352–3355 (2003).
36. DeLano, W.L. *The PyMOL Molecular Graphics System* (DeLano Scientific, San Carlos, California, USA, 2002).